High Efficiency Megawatt Machine Rotating Cryocooler Conceptual Design

Rodger W. Dyson[1] and Ralph H. Jansen[2]
NASA Glenn Research Center, Cleveland, Ohio, 44135, USA

Kirsten P. Duffy[3]
University of Toledo, Toledo, Ohio, 43606, USA

Paul J. Passe[4]
Vantage Partners, Brookpark, Ohio, 44142, USA

Some of the challenges associated with developing electric aircraft propulsion systems include developing powertrain components that are both efficient and light-weight. In particular, electric motors must simultaneously achieve high efficiency by minimizing electrical and mechanical losses while also achieving high specific power by increasing the torque and/or speed. Normally, increasing torque or speed will increase electrical and mechanical losses. The High Efficiency Megawatt Machine (HEMM) minimizes electrical losses by incorporating a superconductor to enable increased current on the rotor. The rotor spins in a vacuum to minimize thermal and mechanical losses. Some organizations have been developing superconducting rotors for similar reasons using either cryogenic fluid transfer systems, fully immersed cryogenic cooling, and in a few cases, built-in cryogenic cooling on the rotor using a Brayton or Stirling system; however, the implementation was too large or inefficient for effective motor integration. Instead, a new approach for cryogenically cooling the superconducting rotor coil with an embedded rotating cryocooler is presented that fits completely within the rotating shaft.

I. Nomenclature

A_x	=	piston maximum amplitude of oscillation
V_x	=	piston maximum velocity amplitude of oscillation
V	=	linear machine coil voltage
C_f	=	motor constant
Fp	=	force on the piston
I	=	linear machine coil current
P	=	power
f	=	oscillation frequency

II. Introduction

Electric aircraft propulsion improves the performance of vehicles by either increasing the effective turbofan by-pass ratio, reducing drag with boundary layer acceleration, or increasing lift with improved wing circulation patterns. All of these benefits require electric motors to move air in strategic ways. But to achieve a net aircraft benefit it is also

[1] Hybrid Gas Electric Propulsion Technical Lead, Thermal Energy Conversion Branch
[2] Technical Integration Manager, Aeronautics Mission Office, Member
[3] Senior Research Associate, Rotating and Drive Systems Branch, Member
[4] Mechanical Designer, Mechanical Engineering Department

crucial for the added motors to be highly efficient and light-weight. For many years, it was assumed superconducting technologies would be required to achieve the necessary efficiency and mass goals. The challenge has always been two-fold: 1). how to achieve cryogenic temperatures inside the motor; and 2). how to use alternating current in a superconductor. The HEMM provides a compromise solution between a fully superconducting machine and a fully ambient machine.

Ambient machines achieve high specific power by increasing speed until structural, thermal, or dynamic stability limits are reached while keeping the efficiency reasonable through careful selection of materials, magnetic field orientation and frequency in the back-iron and/or use of air-core designs, effectively trading torque current density for speed. Permanent magnet rotor machines dominate in this category. Examples of this approach include the University of Illinois high speed permanent magnet machine[1-2]. These approaches work well for achieving machines in the 95-97% efficiency range with a specific power below10 kw/kg (including full mass accounting of active magnetics and support structures). Indeed, this class of machine is enabling the first generation of electric aircraft and does not have any of the challenges associated with incorporating cryogenic liquids or coolers on aircraft.

Fully superconducting machines in which both the rotor and the stator incorporate superconducting coils offer the highest potential efficiency and specific power machine if the cooling system mass is managed and the superconducting alternating current losses are minimized. Utilizing cryogenic fuels is a natural option for providing on-board cooling but have the drawback of requiring more volume per unit energy than jet fuel and only liquid hydrogen is currently cool enough for AC loss mitigation using MgB_2 superconductors. The cost of producing and supporting LH_2 at airports and in aircraft and the additional aircraft drag from the required larger airframes are some considerations to address before this approach can be competitive.

A compromise between ambient and fully superconducting machines is partially superconducting on the rotor DC wound field coil only. This allows for maximizing the air gap magnetic field using a direct current field on the rotor while operating the stator at ambient temperatures with AC current. This approach has been investigated in the past using three common approaches[2]. First, cooling the rotor with a cryogenic fluid that is delivered through a rotating seal. Second, cooling the rotor with an embedded Brayton cycle. Third, cooling the rotor with an embedded Stirling pulse-tube cycle. All these approaches have been met with mixed success due to integration and efficiency challenges. The Stirling pulse-tube approach worked well up to speeds of 1400 RPM before vibration became an issue and the large diameter of the system precluded direct installation into the rotor shaft.

The HEMM improves upon the previous Stirling pulse-tube approach by co-optimizing the linear machine and pulse-tube cooler so they fit inside a 100mm hollow rotor shaft[3, 4]. The benefit of this approach is it enables machine compactness and high thermal isolation of the rotor. The compactness was achieved by optimizing a Redlich style linear machine with a co-axial pulse-tube cooler into a slender device that can lift 50W at 50K from the rotor and reject both the linear machine, compressor, and cryogenic heat load to ambient.

The remaining balance of this paper will detail the rotating cryocooler design parameters for a 1.4 MW electric machine. And finally, some discussion about the motor scalability and range of superconducting temperatures that could be achieved with this design approach will be provided.

III. HEMM Interface Requirements.

Typically, machines have to trade specific power and efficiency; however, both are crucial for a successful design[5-6]. The HEMM has the potential to achieve high specific power and efficiency goals simultaneously because it utilizes superconducting wires in the rotor, which provide a much higher air gap field capability than either permanent magnets, normal wound field conductors, or an induction rotor configuration. Employing superconducting coils provides a dramatic improvement in magnetic field generated because the direct current resistance is zero in the superconductor at the correct operating conditions. However, superconducting machine applications have been limited because superconductors require cryogenic temperatures to operate, which typically require a separate cryogenic fluid cooling system, adding mass, volume, and complexity to the overall system.

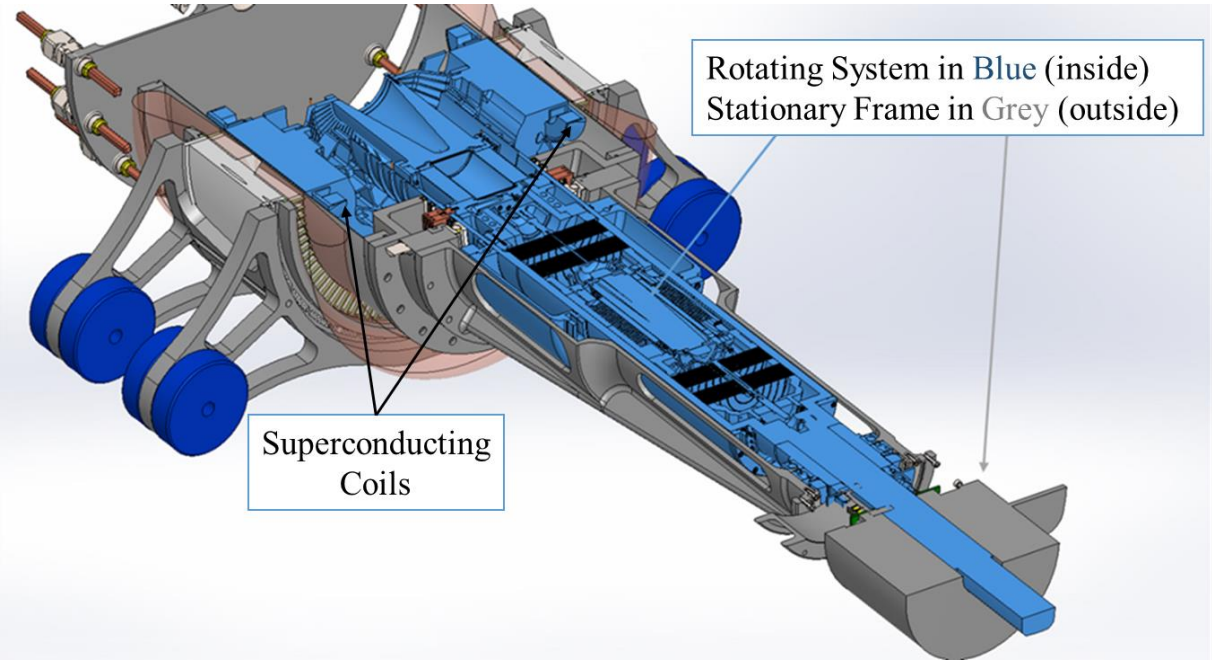

Figure 1. High Efficiency Megawatt Motor (HEMM) Cross-Section

The HEMM incorporates a cryocooler in the rotor of the machine as shown in Fig. 1, and connects the cold tip of the cryocooler to the superconducting coils conductively, thereby eliminating the need for any external cryogenic equipment or any cryogenic fluids. The machine's internal cryocooler has been designed to lift 50W of heat from a 50K cold tip and reject to a 300K ambient environment. This cryocooler is also intended to be light weight (<10kg), small diameter (<100mm), and capable of withstanding 6800RPM rotation about its central axis such that it can be integrated into the shaft of the HEMM. Incorporation of the cryocooler and its related subcomponents within the motor will enable the HEMM to interface with the aircraft in the same way as any standard electric machine, avoiding the additional mass, volume, and infrastructure which would be required with a traditional superconducting machine.

A summary of the loss estimation at rated operating conditions is shown in Table 1. Electromagnetic losses were calculated using a combination of a commercial motor sizing code and spreadsheet calculations for stator winding proximity losses. The proximity losses in this machine are significant, because the stator winding is directly exposed to a significant AC magnetic field imposed by the rotor field. As a result, Litz wire is required to minimize these losses, at the expense of copper packing factor in the stator.

Table 1. Cryocooler Heat Loads

Component	Loss (kW)
Electromagnetic Losses	9.3
Stator Core	3.9
Stator winding (I^2R)	4.6
Stator winding proximity	0.8
Rotor core	0.009
Rotor coils	0
Other Losses	4
Cryocooler Power	2
Bearings	1
Vacuum Seals	1
Total Losses	13.5
Total Losses(+20% margin)	16.2

Other losses were calculated using a combination of in-house codes for cryocooler power estimation, and spreadsheet calculations for proximity and bearing losses. Additional losses were calculated separately to account for the total loss in the machine. The estimated total losses are 13.5kW, comprised of 9.3kW electromagnetic loss, 1kW due to bearing drag, 2.5kW to power the cryocooler, and 1kW due to seal drag. A 20% loss estimate margin is added to account for design and analysis uncertainties, resulting in a total loss with margin of 16.2kW. Also, by increasing the number of phases of the stator windings, the amount of magnetomotive force harmonics produced in the rotor is limited, which thereby limits the amount of heat loss in the rotor. And other features

such as rotating in a vacuum, low emissivity coatings, and thin torque conduction paths minimize the total heat the cryocooler must lift.

In particular, note that the direct (rotor core and coil) and induced parasitic losses (stator radiation, windage loss thermal convection, penetration heat leakage conduction) on the rotor must be kept below 50W for the cryocooler to maintain a 50K cold finger temperature. The temperature at the rotor Rare-Earth barium copper oxide (REBCO) superconducting windings must be kept below 63K. If the amount of heat loss in the rotor is less than the amount that can be lifted by the cryocooler then the cryocooler will be able to operate to sufficiently cool the rotor windings to cryogenic superconducting temperatures.

IV. Cryocooler Trades

A number of different cryocooler configurations were considered for this application. Note that the cryocooler design as shown in Fig. 2 consists of the following components: a linear machine to convert electric power into mechanical force; a piston that converts the mechanical force into an oscillating pressure wave; and a thermo-acoustic circuit to convert the acoustic pressure wave into a no moving part cryogenic heat pump. The last section shown is an example thermal bridge that conductively cools the rotor.

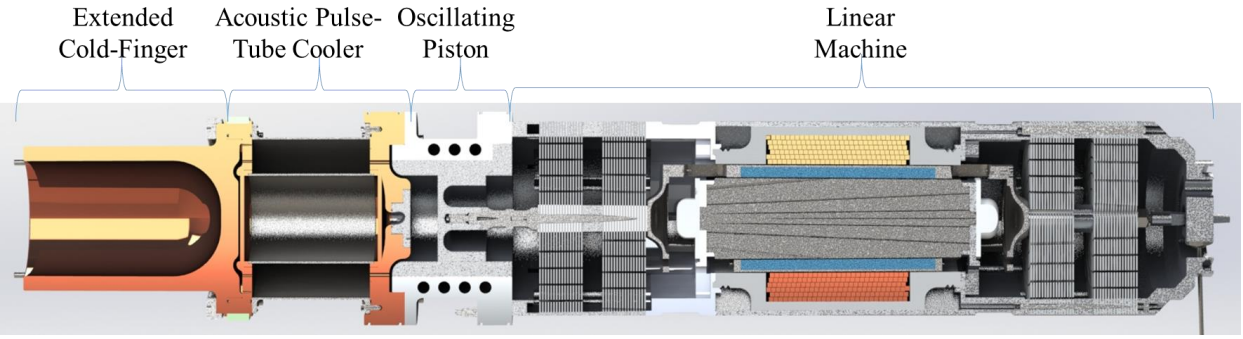

Figure 2. Cryocooler Segments

As summarized in Fig. 3, there are a wide variety of choices for the cryocooler components that were considered but the Redlich style linear machine with flexure bearings and a no moving part single-stage pulse-tube cryocooler was selected. The primary reasons for this selection include:

- Overall design is axisymmetric for dynamic stability under rotation
- Redlich style permanent magnet linear machine increases force with axial length increases (high aspect ratio)
- No cold moving parts or bearings
- Single tight-clearance seal that can be supported with many radially stiff flexure bearings
- Fits within 100mm diameter torque tube
- Can be designed to lift 50W at 50K with reasonable efficiency and size
- Thermal rejection can be located outside the vacuum enclosed rotor area

It should be noted that this cryocooler configuration can support up to 40K temperature at the cold-finger. If lower temperatures are required, a multi-stage pulse-tube cooler would be utilized.

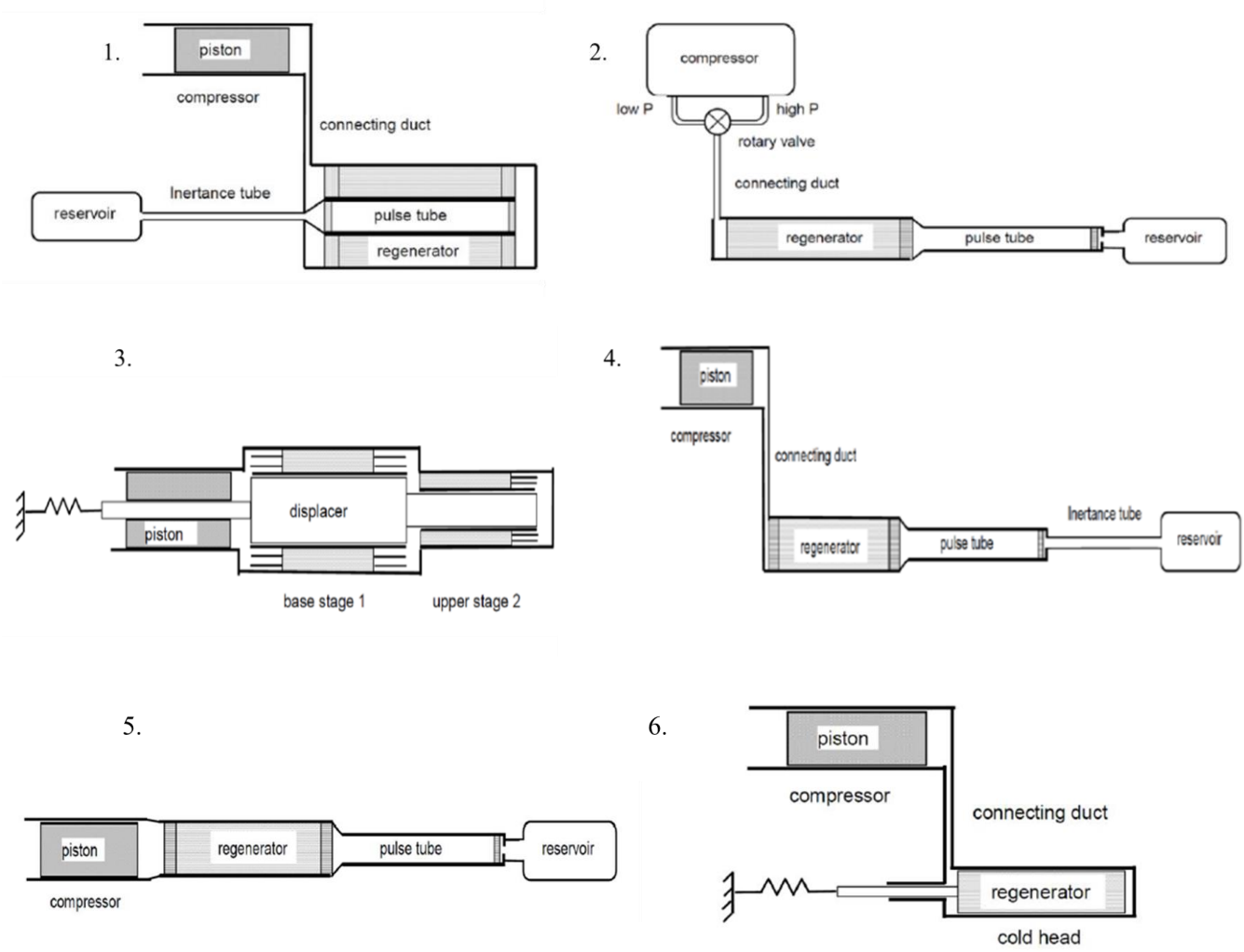

Cryocooler Type	Property
1. Co-axial Pulse Tube	Efficient enough and fits in rotating shaft
2. GM-Pulse Tube	Not Efficient
3. Two-Stage Stirling Displacer	Very efficient, but challenging to rotate displacer
4. Inline Pulse Tube	Too long vs. Co-axial
5. Pulse Tube	Not as efficient as two-stage, Too long
6. Split Cycle	Not axi-symmetric for high speed rotation

Figure 3. Thermo-Acoustic Heat Pumping Options Considered

A. Linear Machine

The linear machine converts electric AC power input into mechanical oscillating power that drives a tight clearance piston to create high intensity acoustic waves to power the pulse-tube cooler. A wide range of linear machines was considered for this purpose including the STAR configuration, moving iron configuration, and moving coil

configuration. The STAR[7] configuration was attractive because of the inherent magnetic spring stiffness but the radial flux path resulted in a short and wide system that cannot fit within the narrow dimensions of the rotating shaft. The moving iron configuration would result in a heavier system that reduces machine specific power. The moving coil configuration was not considered due to the oscillating and rotating forces that would be imposed on it.

Instead, a Redlich linear machine[8] configuration was selected as shown in Fig. 4 and optimized for both efficiency, dimensional compatibility, and impedance matched to the cryocooler. Until recently, linear machines were optimized and built separately from the pulse-tube cooler because of analytical limitations of combining electromagnetic physics with thermo-acoustic physics. Separate optimizations would result in impedance matching challenges that require iterative re-optimization of both systems before a compatible system could be found. That approach is problematic when trying to embed an entire cryocooler inside a relatively small diameter shaft because the number of design constraints is very large and disconnected. Instead, a combined approach of simultaneously optimizing all the electromagnetic and thermo-acoustic related physical dimensions allows for a gradient based optimized system solution that meets all the constraints. And fortunately, we were able to identify a unique configuration that could meet all the machine integration requirements including fitting in a relatively small diameter shaft. The result is a narrow and somewhat long linear machine that can provide about 1800W of acoustic power for the co-axial pulse cooler.

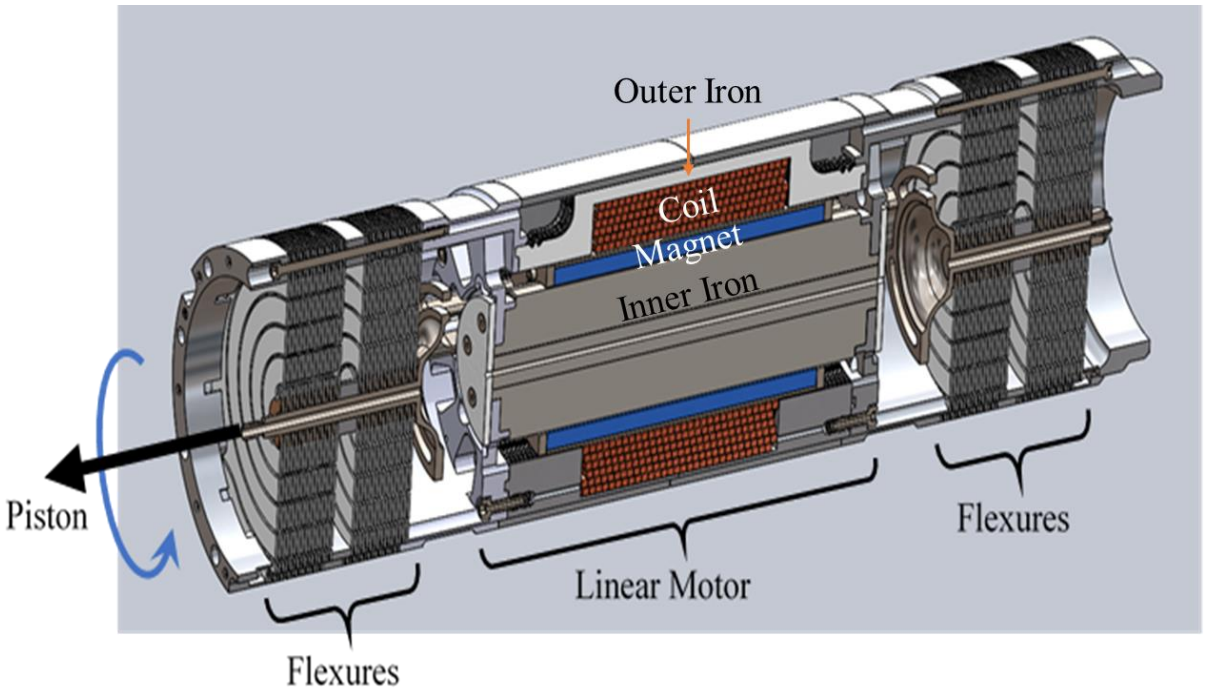

Figure 4 – Linear actuator portion of cryocooler, including flexures

1. *Electromagnetic Design*

The primary challenge of fitting a linear machine in a high aspect ratio space is the magnetic flux gets concentrated in the iron as the power increases or diameter decreases. And once the soft magnetic iron saturates the electric to mechanical power conversion response begins to flatten. It turns out portions of the cycle can magnetically saturate the iron because other forces such as spring flexure and pressure dominate at the extremes of motion. As shown in Fig. 5, the magnetic force is at a minimum when the piston is fully extended (flexure force dominates), and the magnetic force peaks when the piston is at mid-stroke. In the mid-stroke position nearly all the force is due to magnetic field.

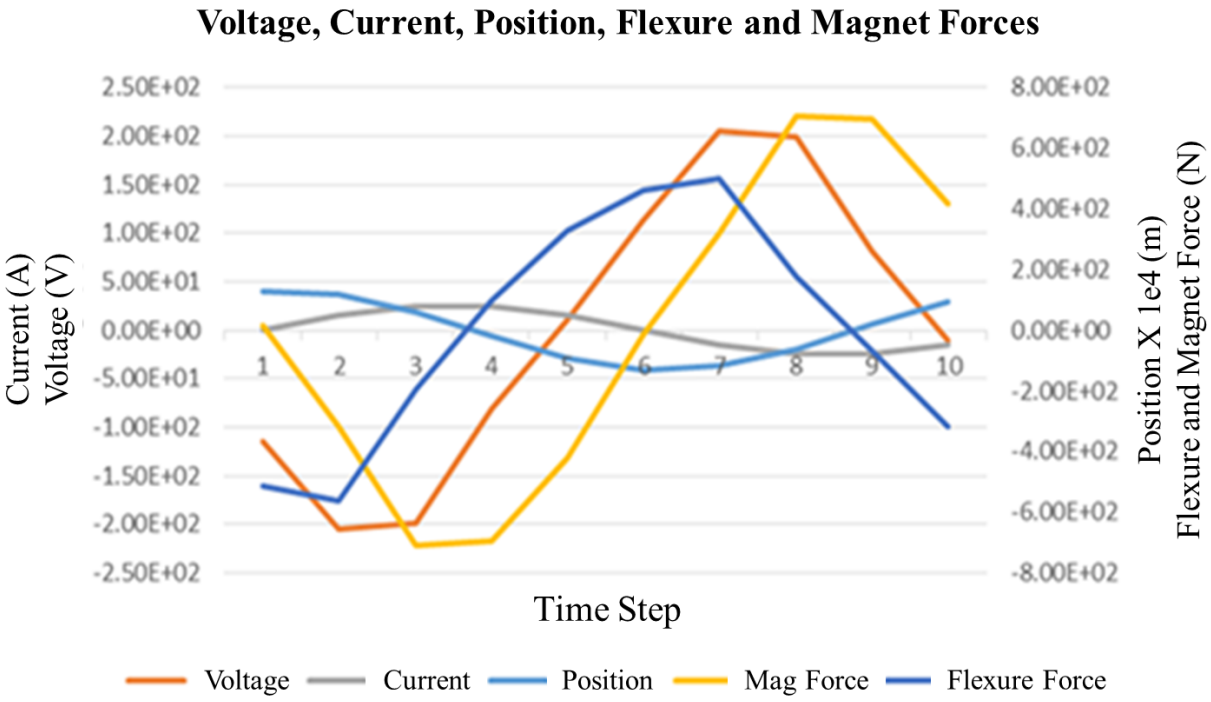

Fig. 5. Mechanical and Electrical Phase Relationships

And shown in Fig. 6 are the forces during a complete cycle acting on the moving permanent magnet. Note that despite the middle section of the magnet not being located near the poles, it is a significant contributor to the overall force acting on the piston.

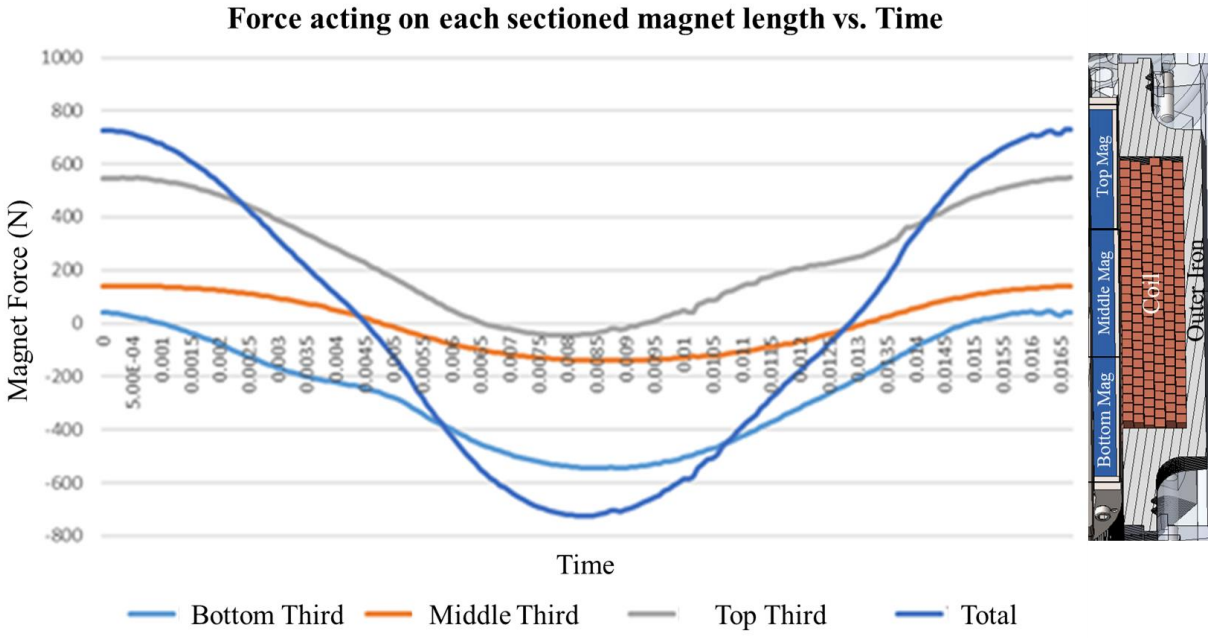

Fig. 6 Magnetic forces acting on the top third, middle third, and bottom third

This means we can lengthen the linear machine to achieve higher overall power delivery even when the soft iron starts to saturate. Notice also at the end-strokes that the top and bottom magnetic forces cancel and the middle of the magnet has no magnetic forces acting on it. We can also increase the frequency of the machine to further increase power delivery without increasing soft magnetic iron in a small diameter shaft:

$$F_p = C_f\, I \tag{1}$$

$$P = F_p V_x = VI \tag{2}$$

And after combining equations (1) and (2) we find:

$$V_x C_f = V \tag{3}$$

$$V_x = A_x\, 2\, \pi\, f \tag{4}$$

So by increasing frequency, we can increase power without increasing current. This way, while the soft magnetics may saturate during a portion of the cycle, the higher frequency keeps the saturation at the same level while delivering more power per cycle. These results imply that the linear machine's delivered power can be increased by increasing frequency and magnet length while maintaining a small overall diameter. In addition, if the amplitude of oscillation could be increased, this would also increase the specific power; however the small diameter limits the allowed deflection of the flexure bearings. While increasing the frequency is desirable electromagnetically, the strength of the flexures must be increased to support the higher axial forces and the pulse-tube cooler prefers to operate at lower frequencies due to thermal transfer rate limits. These constraints are explained further below and result in a system that optimizes around 60 Hz.

B. Mechanical Design

Within the cryocooler is an oscillating piston that drives acoustic waves at approximately 60 Hz. This piston is driven by a linear motor, and the piston shaft is held by a series of flexures (see Figure 4) that provide a prescribed axial stiffness and moving mass. The flexure design is challenging, because the oscillating amplitude of 13mm is relatively large compared to the outer diameter of 100 mm, in fact the larger the amplitude the better the cryocooler is expected to perform. In addition, the cryocooler needs to function both at rest and at 6800 RPM.

1. Flexure Bearings

A flexure design with spiral arms was created in order to give a particular stiffness value at the maximum axial displacement, and a particular moving mass. The original flexure design had arms that deflected too far radially during the 6800 RPM rotation, so that adjacent arms would be in contact. A new design was created without this problem, and with a material thickness of 0.8 mm (0.0315 inches). A total of 64 flexures are required to give the axial stiffness required. The 64 flexures are positioned as 4 sets of 16 flexures, with 2 sets on either side of the linear motor as shown in Figure 4. Each group of 2 sets has flexures that are oriented in opposite directions. Between the flexures are spacers on the outer diameter, and bushings on the inner diameter, so that adjacent flexures will not be in contact during motion. One of the benefits of using a relatively large number of flexures is each flexure can be deflected further since it experiences less stress and the high number of flexures significantly increases the radial stiffness on the shaft. These two features are key to maximizing the motor PV mechanical power input to the cooler while under rotation in a narrow shaft.

Figure 7 shows a model of the flexure with its associated spacer and bushing. Table 2 gives the basic properties of the flexure's spirals.

A high-fatigue-strength 420 stainless steel material was chosen for the flexures. The flexure slots are cut with a water knife, and then the flexures are tumbled and shot-peened to introduce compressive stresses into the material surface. Table 3 shows the material properties prior to shot-peening.

Table 2. Flexure Properties

Property	Value
Number of arms	3
Outer diameter	100 mm
Number of revolutions in a spiral arm	1.3
Spiral inner diameter (without stress relief)	20 mm
Spiral outer diameter (without stress relief)	85 mm
Spiral pitch	25 mm
Arm width	6.98 mm
Slot width	1.0 mm

Note that the inner portion of the flexure in Fig. 7 has a straight region to prevent rotation of the shaft that is separate from the flexure. And axially adjacent flexures are installed on the shaft with opposite orientations to not favor a particular rotational mode. Spacers are used between each flexure to insure the arms do not collide during oscillation.

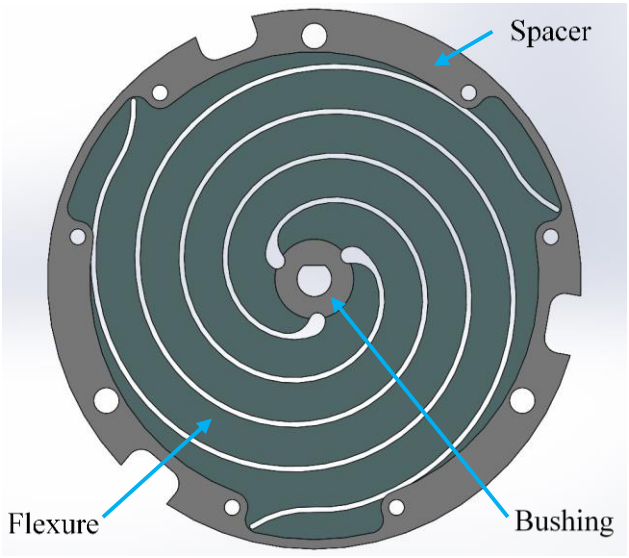

Figure 7 – Flexure geometry

Table 3. Material Properties

Property	Value
Tensile Strength (MPa)	1900
0.2% Yield Strength (MPa)	1500
Fatigue Strength (MPa) 5% Failure Rate	±750
Young's Modulus (GPa)	210
Density (kg/m^3)	7700

Both finite element analysis (FEA) and flexure specimen testing were used to determine the axial stiffness and moving mass of the flexure design, and results are shown in Table 4. These test results for stiffness and moving mass values are acceptable for the cryocooler design.

Table 4. Single flexure stiffness and moving mass

Property	0 RPM Test (n=3 samples)	0 RPM FEA prediction	6800 RPM FEA prediction
Stiffness (N/m) at 13 mm displacement	2642	2601	2937
Moving mass (g)	17.0	16.3	16.5

Since the axial displacement is quite large, a stress analysis needed to be done to determine the maximum mean and alternating stress in the flexure during operation. Figure 8 shows results for the von Mises stress and deformation for the flexure at 6800 RPM and 13 mm axial displacement. There are high stress areas at each end of the flexure arms, with the maximum of 497 MPa near the inner diameter. This maximum occurs on the face of the flexure.

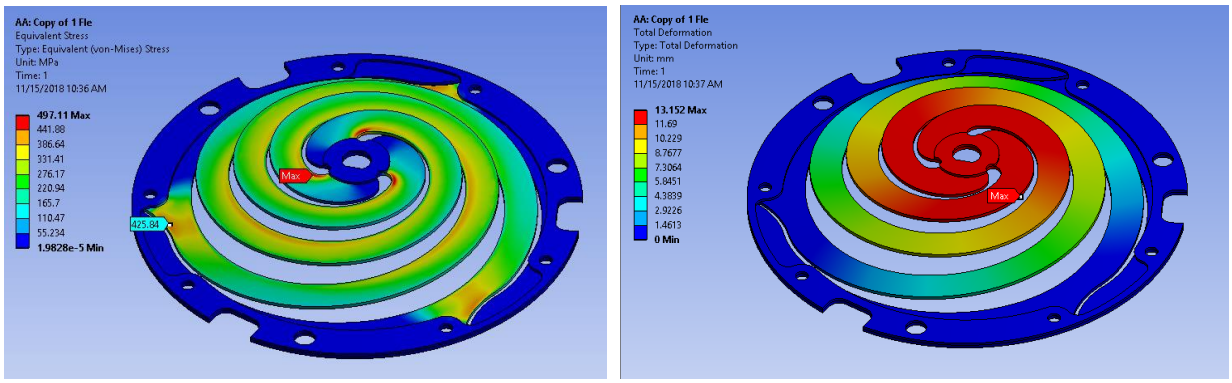

(a) Von Mises stress **(b) Deformation (13 mm axial)**

Figure 8 – Results for 6800 RPM and 13 mm axial displacement

Figure 9 shows the modified Goodman line for the flexure at 13 mm displacement, and at 0 RPM and 6800 RPM. The line assumes a 1.33 factor of safety on fatigue strength, 1.1 factor of safety on yield strength, and 1.5 factor of safety on ultimate tensile strength. The strengths are for the material prior to shot-peening. The margin shown is 29.3% at 0 RPM and 11.2% at 6800 RPM.

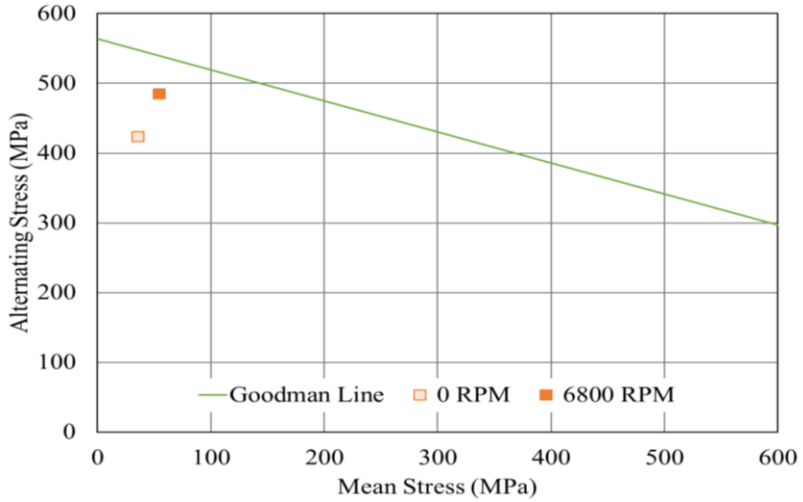

Figure 9 – Modified Goodman line for flexure at 13mm displacement and 6800 RPM

V. Pulse-tube Cooler

The linear machine oscillates a piston in a helium working fluid with non-contacting clearance seals to drive a pulse-tube cooler. Traditionally, a Stirling displacer-type cooler would be used due to having high efficiency; however in this rotating system the additional side-loads on the displacer introduce more risk that the displacer would rub when simultaneously oscillating and rotating at cryogenic temperatures. Instead, an acoustic Stirling configuration is used that leverages inertial properties of the working fluid to achieve the proper pressure and volume velocity phasing in the regenerator.

A. Acoustic Circuit Design

As shown in Fig. 10, the selected cooler design is based on acoustic pulse-tube technology. Note the oscillating piston creates a traveling acoustic wave that initially travels around the inner pulse tube through the regenerator where with proper pressure and volume velocity phasing is enforced and forms an acoustic heat pump that lifts heat from the left-side copper heat exchanger at 50K to the right side copper heat exchanger at 353K. The remaining acoustic energy then travels through the pulse-tube which acts like a Stirling displacer and the remaining energy then travels down the inertance tube that surrounds the piston (in the piston bore) which then terminates in the reservoir as highlighted in Fig. 11. Note that this coaxial configuration enables the entire cryocooler to be installed inside the rotating torque tube of the machine. All of the cold regions are inside the thermally isolated vacuum region while all the rejecting ambient regions are outside the rotor vacuum region. The only tight clearance is the single moving piston that is supported with 64 flexure springs as shown to the right in Fig. 10.

Previous analysis has confirmed that rotating a pulse-tube cooler horizontally should not impact the performance of the system[2]. But even so, the pulse-tube aspect ratio would ideally be higher to minimize streaming effects and radiation losses. Extending the length also comes with a performance cost so the current length is a balance between these various potential losses.

The other challenge associated with this rotating cryocooler is the potential for regenerator blow-by due to the centrifugal forces. Initially a random fiber regenerator with 77% porosity and 12 micron diameter fiber will be employed that is tightly packed to prevent blow-by under rotation.

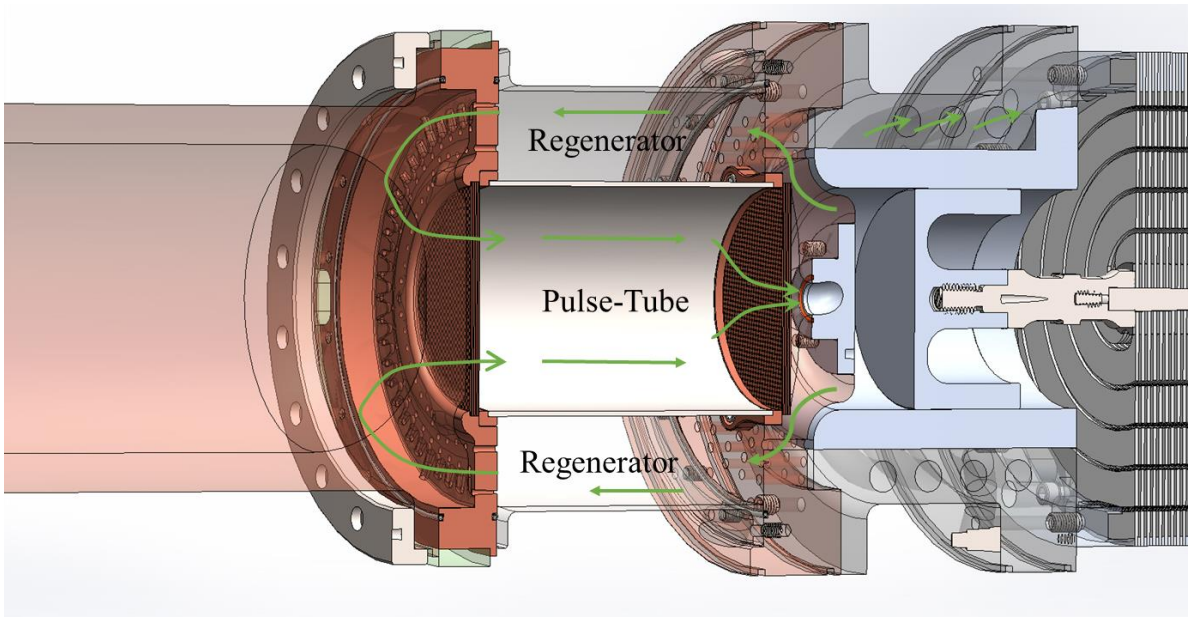

Fig. 10 Acoustic Pulse-tube Cryogenic Cooler Flow Path

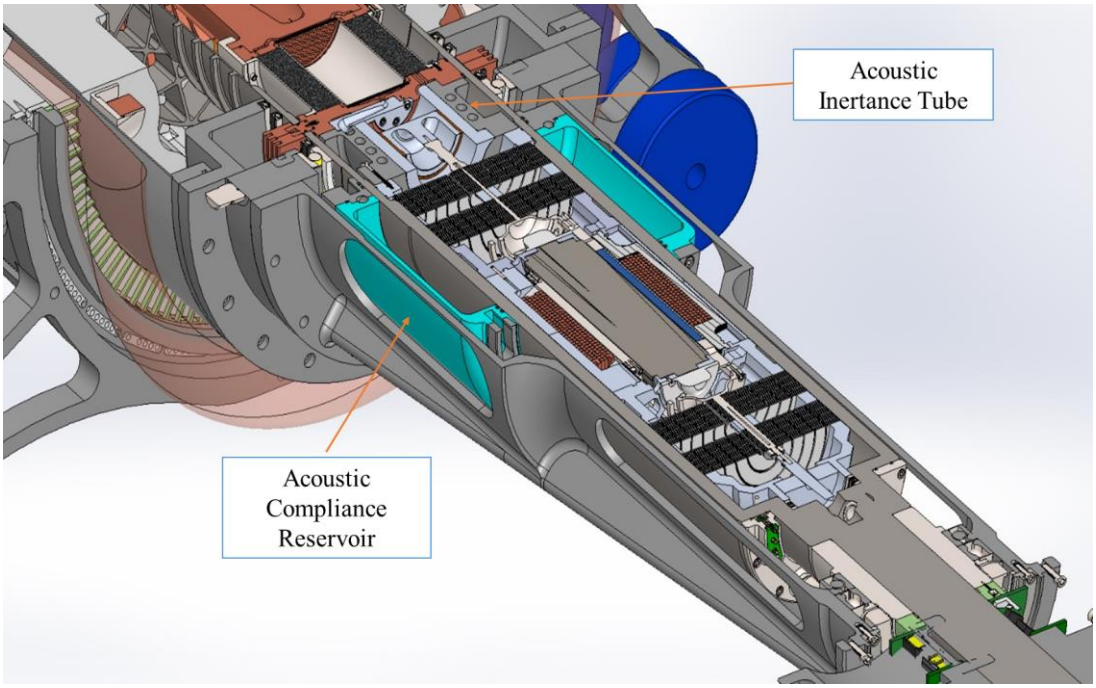

Fig. 11 Highlighted region is the acoustic reservoir at the end of the inertance tube

VI. Control and Operation

As discussed in Section 4B, the cryocooler must operate when the electric machine is rotating and stationary, but this changes the mechanical stiffness of the flexure bearings which in turn changes the resonant frequency of the mechanical system. There are two ways to manage this:

1. Change the operating frequency by approximately 6 Hz to maintain the same operating characteristics.
2. Change the reactive power in the coils while maintaining a fixed oscillation frequency, in effect having the power supply provide additional spring force magnetically. The operating parameters of this approach are shown in Table 5.

Table 5. Stationary and Rotational Operating Parameters

Property	**0 RPM**	**6800 RPM**
Piston Oscillation Freq (Hz)	**56**	**56**
Heat Lifted at 50K (W)	**51**	**51**
Electric Power In (W)	**1860**	**1774**
Effective Flexure Stiffness (N/m)	**1.57e5**	**1.78e5**
Reactive Power In (W)	**2531**	**3121**
Voltage (V)	**154**	**176**
Current (A)	**20.4**	**20.4**
Power Factor	**0.59**	**0.49**

Note that the reactive power required is higher under rotation, but the real power input is minimized. The overall current is kept the same, but the phase difference between the voltage and the current differs under rotation.

A. Cooling Rates

As shown in Fig. 12, the amount of heat the cryocooler can lift under full power input varies as the cold-finger temperature changes. This is important because in a practical machine on aircraft we need to minimize the preparation time between flights. The rotor superconductor cannot be operated until cryogenic temperatures are reached. But the thermal mass of the system can be significant. Once the system steady cryogenic temperatures are reached, then the cryocooler only has a modest 50W at 50K to lift.

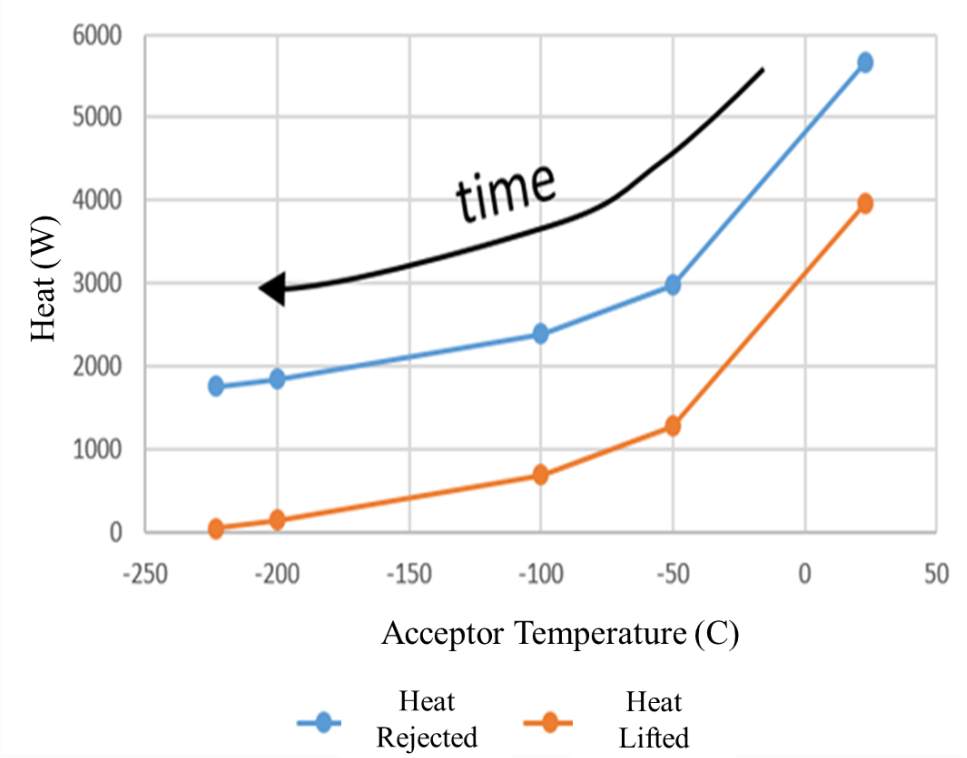

Figure 12. Typical Heat Lift and Rejection Curve vs. Time and Temp

Note that the electric input power stays constant (1800W), but since the heat lifted increases with temperature, then so does the heat rejected. At ambient temperatures, approximately 5500W is being reject (4000W lifted), below 173K the amount of heat lifted begins to drop significantly.

B. Performance Validation

The cryocooler will need to operate under a range of conditions including stationary and rotating up to 6800 RPM, and typically under full power conditions since cooling at the fastest rate possible is desirable. To ensure that the flexures will survive, they will be tested in the linear motor subassembly at the ±13 mm oscillation amplitude for approximately 10^7 cycles, first at 0 RPM, and then at 6800 RPM as shown in Fig. 13. Moreover, this test rig will confirm the piston does not rub and that the proper cryogenic temperature of 50K is achieved in the thermally isolated cold-finger while lifting 50W of thermal heat.

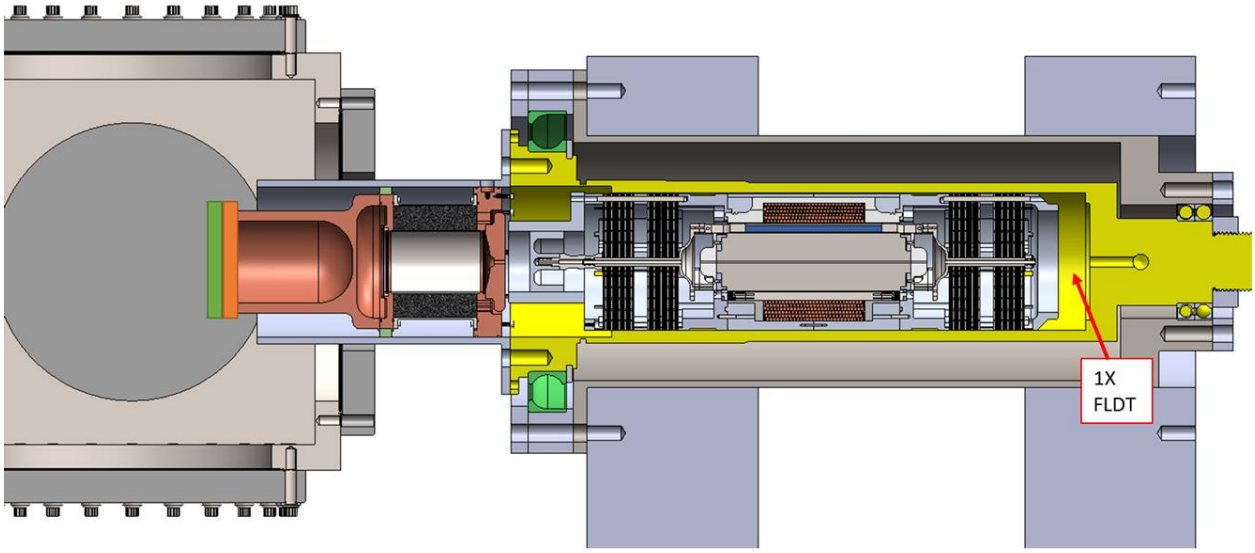

Figure 13. Cryocooler flexure qualification and vacuum isolated cold-finger heat pump test

The yellow structure shown in Fig. 13 rotates with the cryocooler and while transferring machine torque to the right. Power is delivered to the cryocooler via slip rings initially for this test, and a brushless rotary transformer is planned to be used in a later version.

VII. Summary

If the rotating cryocooler described herein is successful it will greatly simplify the implementation of partial superconducting coils on the wound field rotor. Industry standard design tools that have previously been extensively validated have confirmed this machine should work well and it is expected to achieve over 16 kw/kg active magnetic circuit mass and over 98% efficiency when rotating at 6800 RPM and generating 1.4MW of electric power. A cryocooler risk reduction prototype is currently being constructed and will soon be tested under full speed rotation to confirm its operation.

It is not obvious that the electrical, mechanical, thermal, dimensional, material, operational, and acoustical requirements of this integrated machine can all be met to form a practical partially superconducting 1.4 MW machine. But after extensive analysis it appears we have a machine design that should work well. More details of this integration accomplishment can be found in references by Jansen, Woodworth, and Scheidler[9-12] and the next step is to build and fully test the prototype.

Acknowledgments

This work is supported by both the AATT Project and the CAS HEATHER Project. A team with a broad skill set is required to design, build, and test a fully integrated partially superconducting machine. The team members include: Aaron Anderson, Thomas Balogas, Dr. Kirsten Duffy, Dr. Rodger Dyson, Don Fong, Hardy Hartman, Hashmatullah Hasseeb, George Horning, Frank Gaspare, Scott Metzger, Wesley Miller, Paul Passe, Malcolm Robbie, Dr. Justin Scheidler, Andrew Smith, Erik Stalcup, Will Sixel, Casey Theman, Tom Tallerico, William Torres, and Dr. Andrew Woodworth

VIII. References

1. Kiruba S Haran, Swarn Kalsi, Tabea Arndt, Haran Karmaker, Rod Badcock, Bob Buckley, Timothy Haugan, Mitsuru Izumi, David Loder, James W Bray, Philippe Masson and Ernst Wolfgang Stautner, "High power density superconducting rotating machines—development status and technology roadmap", Superconductor Science and Technology, Volume 30, Number 12, https://nari.arc.nasa.gov/sites/default/files/Haran_LEARN_Seminar%281%29.pdf
2. "Development of Ultra-Efficient Electric Motors", RELIANCE ELECTRIC COMPANY, May 2008, Development of Ultra-Efficient Electric Motors DoE Cooperative Agreement No. DE-FC36-93CH10580, https://www.osti.gov/servlets/purl/973932,
3. Dyson, R.W., Wilson, S.D., Tew, R.C., Demko R., "Fast Whole-Engine Stirling Analysis", AIAA-2005-5558, 3rd International Energy Conversion Engineering Conference, San Francisco, CA, 2005
4. Dyson R.W., Geng, S. M., Tew, R.C., Adelino, M., "Towards Fully Three-Dimensional Virtual Stirling Convertors For Multi-Physics Analysis and Optimization", Engineering Applications of Computational Fluid Mechanics, Vol. 2, No. 1, 2008
5. Ralph H. Jansen, Dr. Peter Kascak, Dr. Rodger Dyson, Dr. Andrew Woodworth, Andrew D. Smith, Dr. Justin Scheidler, Thomas Tallerico, Yaritza De Jesus-Arce, David Avanesian, Dr. Kirsten Duffy, Paul Passe, Gerald Szpak, "High Efficiency Megawatt Motor Preliminary Design", *2019 AIAA/IEEE Electric Aircraft Technologies Symposium*, Indianapolis, Indiana, 2019.
6. Jansen, R. H., De Jesus-Arce, Y. , Kascak, P. E., Dyson, R. W., Woodworth, A. A., Scheidler, J. J., Edwards, R. D., Stalcup, E. J., Wilhite, J. M., Duffy, K. D., Passe, P. J., McCormick, S. P., "High Efficiency Megawatt Motor Conceptual Design," 2018 Joint Propulsion Conference, AIAA Propulsion and Energy Forum, AIAA 2018-4699, Cincinnati, Ohio, 2018.
7. Corey, J.B. W., Yarr, G., "HOTS to WATTS: The FPSE Linear Alternator System Re-Invented", 1992
8. Redlich, R., Unger, R., van der Walt, N., "Linear Compressors: Motor Configuration, Modulation and Systems", 1996
9. Andrew A. Woodworth, Andrew Smith, William Sixel, Ryan Edwards, Ralph Jansen, Sean McCormick, Malcolm Robbie,]and Gerald Szpak, Paria Naghipour and Euy-Sik Shin, "Thermal Analysis of Potted Litz Wire for High Power Density Aerospace Electric Machines.", *2019 AIAA/IEEE Electric Aircraft Technologies Symposium*, Indianapolis, Indiana, 2019.
10. Scheidler, J., Tallerico, T., Miller, W., Torres, W. "Progress Towards the Critical Design of the Superconducting Rotor for NASA's 1.4 MW High-Efficiency Electric Machine", *2019 AIAA/IEEE Electric Aircraft Technologies Symposium*, Indianapolis, Indiana, 2019.
11. Jansen, R. H., Kascak, P. E., Dyson, R. W., NASA Glenn Research Center, Cleveland, OH, U.S. Provisional Patent, "Wound field synchronous machine", NASA Docket No. LEW 19477, originally filed June 2016.
12. Dyson, R.W., "Novel Thermal Energy Conversion Technologies for Advanced Electric Air Vehicles", 2018 AIAA Propulsion and Energy Forum, AIAA/IEEE Electric Aircraft Technologies Symposium, July 9-11, 2018, Cincinnati, Ohio